HHS Public Access

Author manuscript

Biochem Biophys Res Commun. Author manuscript; available in PMC 2018 October 21.

Published in final edited form as:

Biochem Biophys Res Commun. 2017 October 21; 492(3): 362–367. doi:10.1016/j.bbrc.2017.08.102.

The L530R variation associated with recurrent kidney stones impairs the structure and function of TRPV5

Lingyun Wang[a], **Ross P. Holmes**[b], and **Ji-Bin Peng**[a,b,*]

[a]Division of Nephrology, Department of Medicine, Nephrology Research and Training Center, University of Alabama at Birmingham, Birmingham, AL 35294

[b]Department of Urology, University of Alabama at Birmingham, Birmingham, AL 35294

Abstract

TRPV5 is a Ca^{2+}-selective channel that plays a key role in the reabsorption of Ca^{2+} ions in the kidney. Recently, a rare L530R variation (rs757494578) of TRPV5 was found to be associated with recurrent kidney stones in a founder population. However, it was unclear to what extent this variation alters the structure and function of TRPV5. To evaluate the function and expression of the TRPV5 variant, Ca^{2+} uptake in *Xenopus* oocytes and western blot analysis were performed. The L530R variation abolished the Ca^{2+} uptake activity of TRPV5 in *Xenopus* oocytes. The variant protein was expressed with drastic reduction in complex glycosylation. To assess the structural effects of this L530R variation, TRPV5 was modeled based on the crystal structure of TRPV6 and molecular dynamics simulations were carried out. Simulation results showed that the L530R variation disrupts the hydrophobic interaction between L530 and L502, damaging the secondary structure of transmembrane domain 5. The variation also alters its interaction with membrane lipid molecules. Compared to the electroneutral L530, the positively charged R530 residue shifts the surface electrostatic potential towards positive. R530 is attracted to the negatively charged phosphate group rather than the hydrophobic carbon atoms of membrane lipids. This shifts the pore helix where R530 is located and the D542 residue in the Ca^{2+}-selective filter towards the surface of the membrane. These alterations may lead to misfolding of TRPV5, reduction in translocation of the channel to the plasma membrane and/or impaired Ca^{2+} transport function of the channel, and ultimately disrupt TRPV5-mediated Ca^{2+} reabsorption.

Keywords

TRPV5; Ca^{2+}-selective channel; kidney stone; L530R variation; membrane interaction

[*]To whom correspondence should be addressed. jibinpeng@uabmc.edu.

1. Introduction

TRPV5, one of the two epithelial Ca^{2+} channels with a high Ca^{2+} selectivity, is mainly expressed in the distal convoluted tubule (DCT) and connecting tubule (CNT) in the kidney [1; 2]. It regulates the first step in transcellular Ca^{2+} transport and is considered as a gatekeeper for active Ca^{2+} reabsorption [3]. The knockout of TRPV5 in mice resulted in severe hypercalciuria and bone abnormalities [2]. Furthermore, altered expression of TRPV5 in mouse models of human diseases is associated with vitamin D-deficiency rickets, altered estrogen levels and postmepausal osteoporosis, and parathyroid hormone-related disorders [4].

Several nonsynonymous single nucleotide polymorphisms (SNPs) in TRPV5, including A8V (rs4252372), R154H (rs4236480), A563T (rs4252499) and L712F (rs4252509), have been found in African Americans with high allele frequency [5; 6]. Our previous works indicate that the A563T variation increases TRPV5-mediated Ca^{2+} transport [6] and affects the structure and dynamics of the pore regions of TRPV5 [7]. This variation may contribute to an increased renal Ca^{2+} reabsorption in African Americans compared to Caucasians. The R154H variation, which is present in both African and non-African populations at a relatively high allele frequency, usually causes a lower Ca^{2+} uptake activity in TRPV5 when combined with other variations [6]. However, in most cases, the decrease in Ca^{2+} uptake does not reach statistical significance [6]. Interestingly, this SNP has been found to be associated with the occurrence of multiple stones in a cohort of 365 kidney stone patients in Taiwan [8]. Recently, a L530R variation (rs757494578) in TRPV5 was found to be associated with recurrent kidney stones in 2636 individuals from a founder population in Iceland [9]. This variation introduces a positive charged residue into a hydrophobic region of the pore helix and likely affects the function of TRPV5; however, the effects of this mutation have not been examined. To understand the role of TRPV5 in kidney stone disease, we assessed the Ca^{2+} transport function of the L530R variant by monitoring radiotracer Ca^{2+} uptake in *Xenopus* oocytes. To gain new insights into the structural changes produced in TRPV5 with the L530R variation, we performed molecular dynamic simulations of TRPV5 using the recently published crystal structure of TRPV6 [10], a close homologue of TRPV5 [11; 12]. Our results are expected to provide further evidence for a relationship between genetic variations in TRPV5 and the risk of kidney stone disease.

2. Material and methods

2.1 Ca^{2+} uptake assay

Ca^{2+} uptake by *Xenopus* oocytes was performed as described previously [6; 13]. The animal protocol used in this study was approved by the Institutional Animal Care and Use Committee (IACUC) of the University of Alabama at Birmingham. The L530R variation of TRPV5 was generated using the QuikChange site-directed mutagenesis kit (Stratagene, La Jolla, CA) in the FLAG-tagged human TRPV5 and the mutation was confirmed by sequencing. The capped complementary RNAs (cRNAs) of FLAG tagged TRPV5 with L530 (reference) and R530 (variant) were prepared using mMESSAGE mMACHINE™ SP6 Transcription Kit (ThermoFisher). Oocytes were microinjected with either the reference or the variant cRNA at 12.5 ng/oocyte or water. Oocytes were cultured in 0.5×L-15 solution

and assayed 2 days after injection by radiotracer $^{45}Ca^{2+}$ uptake in standard Ca^{2+} uptake solution. After uptake, oocytes were washed six times and then lysed in 10% SDS solution. Radioactivity of each oocyte was determined using a scintillation counter. Statistical significance is defined as $P < 0.05$ by a Student's t-test.

2.2 Western blot analyses

Lysates were extracted from ten oocytes/group injected with water, L530 or R530 TRPV5 cRNA. Monoclonal anti-FLAG antibody (F7425, 1:1000 dilution) was purchased from Sigma–Aldrich (St. Louis, MO). Appropriate horseradish peroxidase (HRP)-conjugated secondary antibodies (1:10000 dilution) were purchased from Santa Cruz Biotechnology. Chemiluminescence signals were detected using SuperSignal West Pico Chemiluminescent Substrate kit (Pierce Biotechnology, Rockford, IL).

2.3 System modelling

The modeling of human TRPV5 was performed based on the structure of rat TRPV6 using MODELLER 9.13 software [14]. The template of TRPV6 with Ca^{2+} ions was obtained from the Protein Data Bank with an ID of 5IWP [10]. The sequence of TRPV5 used in modeling contains the linker helix (LH) 1–2, pre-transmembrane (TM) helix (pre-S1), TM helices 1–6 (S1–S6), and the TRP domain. The alignment of the human TRPV5 sequence used in the modeling and the corresponding rat TRPV6 sequence is presented in Fig. S1. Since we are only using human TRPV5 in this study, the species will not be specified hereafter. The identity between the sequences is 83.1%, which is much higher than the threshold of 30% that is considered to be reliable for modeling membrane proteins [15]. The modeled TRPV5 tetramer is shown in Fig. 1A. The L530R variation was introduced into all four subunits of TRPV5 using the mutagenesis function of PyMOL [16]. The two TRPV5 systems containing leucine or arginine residues at amino-acid position 530 are denoted as **L530** and **R530**, respectively.

To mimic the membrane environment, the modeled TRPV5 structures were embedded in a lipid bilayer composed of 299 1-palmitoyl-2-oleoyl-sn-glycero-3-phosphocholine (POPC) lipids using CHARMM-GUI membrane builder [17]. Each system (**L530** or **R530**) was then hydrated with a total of 32,854 TIP3P water molecules on both sides of the bilayer. The approximate dimensions of the resultant simulation box were 126 Å × 126 Å × 110 Å along the x, y, and z axes, respectively. Na^+ and Cl^- ions were added to the system to neutralize it and maintain a 150 mM NaCl concentration. The parameters of a FF14SB force field [18] were assigned to the protein, ions, and water molecules, and a FFlipid14 force field [19] was used for POPC lipids.

2.4 Molecular dynamic simulations

To investigate the effect of the L530R variation on the structural change in TRPV5, two 400 ns molecular dynamic (MD) simulations were performed using the AMBER14 simulation package [20]. The simulation protocol is similar to our previous studies [21; 22; 23; 24; 25], and it can be found in the Supplementary Material. Before data analysis, the root mean square deviation (RMSD) for the Cα atoms of TRPV5 was calculated to assess the equilibration of the simulation. Simulation reached an equilibration state after 200 ns in both

L530 and **R530** systems (Fig. S2). Thus, the last 200 ns simulations were used for analyses by using the CPPTRAJ program of AMBER14. The DSSP method was applied to determine whether an amino acid residue belonged to an α helix [26]. The electrostatic potential for TRPV5 was calculated by APBS [27]. The VMD software [28] was used for structure visualization.

3. Results and discussion

In order to understand the effect of the L530R variation on TRPV5, we evaluated the function and expression of TRPV5 using radiotracer $^{45}Ca^{2+}$ uptake in *Xenopus* oocytes and western blot analysis. We modeled the structure of the TRPV5 containing the L530R variant based on the crystal structure of rat TRPV6. The major findings are described below.

3.1 The L530R variation abolishes the Ca^{2+} transport activity of TRPV5

The functional effect of L530R variation on TRPV5 was evaluated by the Ca^{2+} uptake ability when TRPV5 variants were expressed in *Xenopus* oocytes. Compared to the Ca^{2+} uptake observed in oocytes expressing TRPV5 with L530, Ca^{2+} uptake of TRPV5 with R530 was decreased to a level not statistically different from that of water injected oocytes (negative control) (Fig. 1B). This indicates that Ca^{2+} transport activity was totally abolished by the L530R variation. This could result from a lack of expression of TRPV5 R530 protein, a rapid degradation of the protein, a lack of expression of the protein in the plasma membrane, or a defect in transport function. TRPV5 proteins expressed in *Xenopus* oocytes generally exhibit two major bands when assess in western blot: a lower band that is core-glycosylated, and a higher band that is complexly glycosylated. We have shown previously that the complex-glycosylated band is that expressed in the plasma membrane [6]. The western blot analysis showed that the complex-glycosylated band of TRPV5 (band B in Fig. 1C) was significantly reduced by the L530R variation. This suggested that the L530R variation reduced the level of TRPV5 at the plasma membrane. However, the total loss of Ca^{2+} uptake function suggests that the structural change induced by L530R variation may also impair the Ca^{2+} transport function as well.

3.2 The L530R variation damages the secondary structure of TM5

In order to understand the structural changes introduced by L530R variation, the structure of TRPV5 was first constructed by homology modeling using the crystal structure of TRPV6. In the modeled TRPV5 (Fig. 1A), the four aspartate residues at 542 (D542) form a ring in the middle of the pore as a Ca^{2+}-selective filter [7]. Residue L530 is located in the pore helix and points away from residue D542. Since residue L530 is distant from D542, it is not likely that the L530R variation impacts the structure and function of TRPV5 through a direct interaction between residue 530 and residue D542. We therefore investigated whether the L530R variation affects its nearby residues.

In the modeled TRPV5, residue L530 is on the protein surface and is surrounded by hydrophobic residues leucine 502 (L502), tyrosine 526 (Y526) and alanine 505 (A505) (Fig. S3). The L530R variation introduces a positive charge which would alter hydrophobic interactions. To test this proposition, the electrostatic potential maps for **L530** and **R530**

systems were calculated (Fig. 2A). The positive potential is shown in blue, while the negative potential is shown in red. The surface electrostatic potential for residue 530 is labeled in a dotted circle in Fig. 2A. As expected, the electrostatic potential for residue 530 was shifted from neutral (white color for residue L530) to positive (blue color for residue R530). The changed electrostatic potential may directly alter the interaction between residue 530 and the hydrophobic residue L502. Fig. 2B shows that the hydrophobic side chain of L530 interacts with L502; however, the charged side chain of R530 is oriented away and loses contact with L502.

Since residue 530 and L502 are both located in α helix structures (residue 530 in pore helix and L502 in TM helix 5), secondary structure analysis was performed to assess whether the altered interaction can cause structural changes in TRPV5. To this end, the helix occupancy for each residue was calculated from the equilibrated simulation data (Fig. S4). Comparison between **L530** and **R530** systems showed that the helix occupancy did not change for the total helices (54.7% vs. 55.4%), for the pore helix (99.2% vs. 96.7%) and for TM helix 5 (S5) (81.0% vs. 79.2%). However, due to the altered interaction between residue 530 and L502, the helix occupancy for L502 was significantly decreased in monomers 1 and 4 of the L530R tetramer (100% and 99.9% in **L530** vs. 4.3% and 16.2% in **R530**). This altered the helical structure of S5 and divided S5 into two parts (Fig 2B).

3.3 The L530R variation causes a shift of pore helix and residue D542 towards membrane surface

In the membrane environment, residue 530 is exposed to lipid molecules. Thus, the L530R variation would also alter the interaction between residue 530 and lipid molecules. To examine this proposition, radial distribution functions (RDFs) of residue 530 with the phosphorus (P) atoms and the carbon (C) atoms of POPC lipids were calculated (Fig. 3A). RDF calculates the probability of finding specific atoms away from the given atoms in a distance function [29]. It can describe the strength of the interaction between two groups of atoms, as a large peak indicates a strong interaction while a small peak indicates a weak interaction. The RDF results show that P atoms of POPC have a small peak with residue L530 (around 13.8Å), whereas they have two large peaks with residue R530 (around 5.3 Å and 8.9Å). In addition, C atoms of POPC have a slightly larger peak with residue L530 (around 7.8Å) than that with residue R530 (around 9.1Å). To give a clear view of the interaction between residue 530 and lipid molecules, simulation snapshots are represented in Fig. 3B. The hydrophobic side chain of L530 is surrounded by C atoms of POPC, while the charged side chain of R530 is coordinated with the P atoms of POPC (Fig. 3B).

To further study the interaction between residue 530 and membrane lipids, the mass density describing the location of residues along the bilayer normal (z axis) was calculated for residue 530, pore helix, and residue D542 (Fig. 4A). To give a clear view of the positions of residue 530 and pore helix relative to the membrane surface, final simulation structures are represented in Fig. 4B. The cyan dashed lines in Fig. 4A and cyan lines in Fig. 4B are the density peaks of the P atoms of POPC lipids, which indicate the surfaces of the membrane. Results indicate that when the leucine residue at 530 of TRPV5 was replaced by arginine, the residue moved closer to the membrane surface (Fig. 4B) due to the strong interaction

between the arginine residue and P atoms of POPC (Fig. 3A). The movement of residue R530 further raised the pore helix where it is located towards the membrane surface. Furthermore, the residue D542 in the Ca^{2+}-selective filter also shifted towards the membrane surface in the **R530** system.

This study integrated biochemical and computational approaches to investigate the effects of L530R variation on the structure and function of TRPV5. The Ca^{2+} uptake experiments indicated that the L530R variation results in a total loss-of-function in TRPV5. Based on the western blot results, the mutant TRPV5 protein was synthesized, however, the complexly glycosylated form of TRPV5 was dramatically reduced. As we have previously shown that the complexly glycosylated form is the one detected at the oocyte plasma membrane [6], the plasma membrane expression of the variant was likely significantly reduced. While the unglycosylated TRPV5 can still go to the plasma membrane [13], the variant channel was likely defective in Ca^{2+} transport despite reaching the plasma membrane.

The molecular dynamic simulations provided some insights into the aberrant changes that occurred in the structure of TRPV5 with the L530R variation. The most significant change was that the positively charged arginine produced a positive shift in the electrostatic potential in the lipid membrane environment. This not only disrupted the interaction between residue 530 and the hydrophobic residue L502, but also altered the interaction between the transmembrane domains of TRPV5 and the surrounding lipid molecules. L530 in the pore helix was surrounded by Y526 in the same helix and L502 and A505 in TM5. The hydrophobic interactions between these residues may stabilize the overall hydrophobic core helix structures of TRPV5. In the R530 variant of TRPV5, however, the charged residue R530 disrupted the hydrophobic interaction with L502, leading to a damaged secondary structure of TM5 in two of the four monomers. This might impair the core hydrophobic helix structure and result in the misfolding of TRPV5. In addition, the shift of pore helix towards the membrane surface due to the L530R variation may alter the folding of TRPV5 as well. The starting model in the simulation was the properly folded TRPV5, however, it is possible that the majority of R530 variants could not reach this conformation in actuality. If misfolding occurs, the misfolded proteins will not pass the “quality control” in the endoplasmic reticulum and they will not move forward through the trans-Golgi network where complex-glycosylation takes place. Instead, the misfolded proteins will undergo endoplasmic reticulum-associated protein degradation (ERAD) [30]. This could explain the significant reduction in glycosylation complexity in TRPV5 containing R530 as shown in Figure 1C. Given that the L530R variation resulted a total loss of Ca^{2+} uptake function in TRPV5, even if some of the variant TRPV5 proteins reached the plasma membrane, they were likely dysfunctional. The negatively charged phosphate group in lipid molecules attracted R530 residue and brought the pore helix and the Ca^{2+} filter closer to the plasma membrane. The altered interaction between R530 residue and membrane lipids may also contribute to the disruption of the Ca^{2+} transport function of the channel. Together with the potentially altered secondary structure of TM5, the Ca^{2+} transport function of TRPV5 is likely impaired.

The L530R variation is associated with a significantly increased risk of recurrent kidneys stones in a founder population [9]. Knockout [2] or mutation [31] of the TRPV5 gene in

mice results in drastic urinary Ca^{2+} wasting. It is likely the loss-of-function mutation will cause significant hypercalciuria in the L530R carriers in an autosomal dominant fashion similar to what has been observed in mice [31]. Because the mutation is very rare with the minor allele frequency of 0.13% in this founder population, homozygous L530R is unlikely present in this population, and thus the L530R carriers would have one normal TRPV5 allele. Since TRPV5 tetramer is formed as a functional unit, it is expected that the carriers of L530R will have functional homotetramers of "wild-type" TRPV5, heterotetramers of "wild-type" and variant TRPV5, as well as nonfunctional homotetramers of variant TRPV5. This would result in a significant reduction of TRPV5-mediated Ca^{2+} reabsorption in L530R carries. Mice lacking TRPV5 alone do not form kidney stones under normal conditions [32]. However, when the H^{+-} ATPase is also disrupted in the collecting duct, tubular calcium phosphate crystals are formed in the renal medulla [32]. Taken together, it is likely that the reduction of the Ca^{2+} transport function of TRPV5 in L530R variation carriers will result in hypercalciuria. When other environmental or genetic factors are also present, calcium oxalate crystallization and kidney stone formation may occur. This could explain the recently reported association between this loss-of-function variation of TRPV5 and recurrent kidney stones [9].

Supplementary Material

Refer to Web version on PubMed Central for supplementary material.

Acknowledgments

We thank the Alabama Supercomputer Center and Supercomputer facility at the University of Alabama at Birmingham for providing computational resources. This work was supported by the National Institute of Diabetes and Digestive and Kidney Diseases (R01DK072154 and R01DK104924).

Abbreviations

TRPV5	transient receptor potential cation channel vanilloid subfamily member 5
TM	transmembrane
cRNA	capped complementary RNA
MD	molecular dynamics
RMSD	root mean square deviation
POPC	1-palmitoyl-2-oleoyl-sn-glycero-3-phosphocholine
RDF	radial distribution function

References

1. Hoenderop JG, van der Kemp AWCM, Hartog A, et al. Molecular identification of the apical Ca^{2+} channel in 1,25-dihydroxyvitamin D-3-responsive epithelia. J Biol Chem. 1999; 274:8375–8378. [PubMed: 10085067]

2. Hoenderop JG, van Leeuwen JP, van der Eerden BC, et al. Renal Ca^{2+} wasting, hyperabsorption, and reduced bone thickness in mice lacking TRPV5. J Clin Invest. 2003; 112:1906–1914. [PubMed: 14679186]
3. Na T, Peng JB. TRPV5: A Ca^{2+} Channel for the Fine-Tuning of Ca^{2+} Reabsorption. Handb Exp Pharmacol. 2014; 222:321–357. [PubMed: 24756712]
4. van Abel M, Hoenderop JG, Bindels RJ. The epithelial calcium channels TRPV5 and TRPV6: regulation and implication for disease. Naunyn Schmiedebergs Arch Pharmacol. 2005; 371:295–306. [PubMed: 15747113]
5. Akey JM, Eberle MA, Rieder MJ, et al. Population history and natural selection shape patterns of genetic variation in 132 genes. PLoS Biol. 2004; 2:1591–1599.
6. Na T, Zhang W, Jiang Y, et al. The A563T cariation of the renal epithelial calcium channel TRPV5 among African Americans enhances calcium influx. Am J Physiol Renal Physiol. 2009; 296:1042–1051.
7. Wang L, Homes RP, Peng JB. Molecular modeling of the structural and dynamical changes in calcium channel TRPV5 induced by the African-specific A563T variation. Biochemistry. 2016; 55:1254–1264. [PubMed: 26837804]
8. Khaleel A, Wu MS, Wong HS, et al. A single nucleotide polymorphism (rs4236408) in TRPV5 calcium channel gene is associated with stone multiplicity in calcium nephrolithiasis patients. Mediators Inflamm. 2015; 2015:375427. [PubMed: 26089600]
9. Oddsson A, Sulem P, Helgason H, et al. Common and rare variants associated with kidney stones and biochemical traits. Nat Commun. 2015; 6:7975–7983. [PubMed: 26272126]
10. Saotome K, Singh A, Yelshanskaya M, et al. Crystal structure of the epithelial calcium channel TRPV6. Nature. 2016; 534:506–511. [PubMed: 27296226]
11. Peng JB, Chen XZ, Berger UV, et al. Molecular cloning and characterization of a channel-like transporter mediating interstinal calcium absorption. J Biol Chem. 1999; 274:22739–22746. [PubMed: 10428857]
12. Peng JB. TRPV5 and TRPV6 in Transcellular Ca^{2+} Transport: Regulation, Gene Duplication, and Polymorphisms in African Populations. Adv Exp Med Biol. 2011; 704:239–275. [PubMed: 21290300]
13. Jiang Y, Cong P, Williams SR, et al. WNK4 regulates the secretory pathway via which TRPV5 is targeted to the plasma membrane. Biochem Biophy Res Comm. 2008; 375:225–229.
14. Sali A, Blundell TL. Comparative Protein Modeling by Satisfaction of Spatial Restraints. J Mol Biol. 1993; 234:779–815. [PubMed: 8254673]
15. Forrest LR, Tang CL, Honig B. On the accuracy of homology modeling and sequence alignment methods applied to membrane proteins. Biophys J. 2006; 91:508–517. [PubMed: 16648166]
16. The PyMOL. Molecular Graphics System, Version 1.5.0.4. Schrödinger LLC;
17. Jo S, Lim JB, Klauda JB, et al. CHARMM-GUI Membrane Builder for Mixed Bilayers and Its Application to Yeast Membranes. Biophys J. 2009; 97:50–58. [PubMed: 19580743]
18. Hornak V, Abel R, Okur A, et al. Comparison of multiple amber force fields and development of improved protein backbone parameters. Proteins. 2006; 65:712–725. [PubMed: 16981200]
19. Dickson CJ, Madej BD, Skjevik AA, et al. Lipid14: The Amber Lipid Force Field. J Chem Theory Comput. 2014; 10:865–879. [PubMed: 24803855]
20. Case, DA., Babin, V., Berryman, JT., et al. AMBER 14. University of California; San Francisco: 2014.
21. Fancy RM, Wang L, Napier T, et al. Characterization of Calmodulin-Fas Death Domain Interaction: An integrated experimental and computational studyrated Experimental and Computational Study. Biochemistry. 2014; 53:2680–2688. [PubMed: 24702583]
22. Wang L, Peng JB. Phosphorylation of KLHL3 at serine 433 impairs its interaction with the acidic motif of WNK4: a molecular dynamics study. Protein Sci. 2017; 26:163–173. [PubMed: 27727489]
23. Fancy RM, Wang L, Zeng Q, et al. Characterization of the Interactions between Calmodulin and Death Receptor 5 in Triple-Negative and Estrogen Receptor Positive Breast Cancer Cells: An Integrated Experimental and Computational Study. J Biol Chem. 2016; 291:12862–12870. [PubMed: 27129269]

24. Wang L, Pan D, Yan Q, et al. Activation mechanisms of αVβ3 integrin by binding to fibronectin: a computational study. Protein Sci. 2017; 26:1124–1137. [PubMed: 28340512]
25. Wang L, Murphy-Ullrich JE, Song Y. Molecular insight for the effect of lipid bilayer environments on thrombospondin-1 and calreticulin interactions. Biochemistry. 2014; 53:6309–6322. [PubMed: 25260145]
26. Kabsch W, Sander C. Dictionary of protein secondary structure: pattern recognition of hydrogen-bonded and geometrical features. Biopolymers. 1983; 22:2577–2637. [PubMed: 6667333]
27. Baker NA, Sept D, Joseph S, et al. Electrostatics of nanosystems: Application to microtubules and the ribosome. Proc Natl Acad Sci USA. 2001; 98:10037–10041. [PubMed: 11517324]
28. Humphrey W, Dalke A, Schulten K. VMD: Visual molecular dynamics. J Mol Graphics Modell. 1996; 14:33–38.
29. Li F, Wang L, Xiao N, et al. Dominant conformation of valsartan in sodium dodecyl sulfate micelle environment. J Phys Chem B. 2010; 114:2719–2727. [PubMed: 20131883]
30. Vembar SS, Brodsky JL. One step at a time: endoplasmic reticulum-associated degradation. Nat Rev Mol Cell Biol. 2008; 9:944–957. [PubMed: 19002207]
31. Loh NY, Bentley L, Dimke H, et al. Autosomal dominant hypercalciuria in a mouse model due to a mutation of the epithelial calcium channel, TRPV5. PLoS One. 2013; 8:e55412. [PubMed: 23383183]
32. Renkema KY, Velic A, Dijkman HB, et al. The calcium-sensing receptor promotes urinary acidification to prevent nephrolithiasis. J Am Soc Nephrol. 2009; 20:1705–1713. [PubMed: 19470676]

Highlights

- The L530R variation abolishes the Ca^{2+} uptake activity of TRPV5.
- The L530R variation drastically reduces the complex glycosylation of TRPV5.
- The helix structure of transmembrane domain 5 is damaged by the L530R variation.
- The L530R variation shifts pore helix towards the outer surface of plasma membrane.

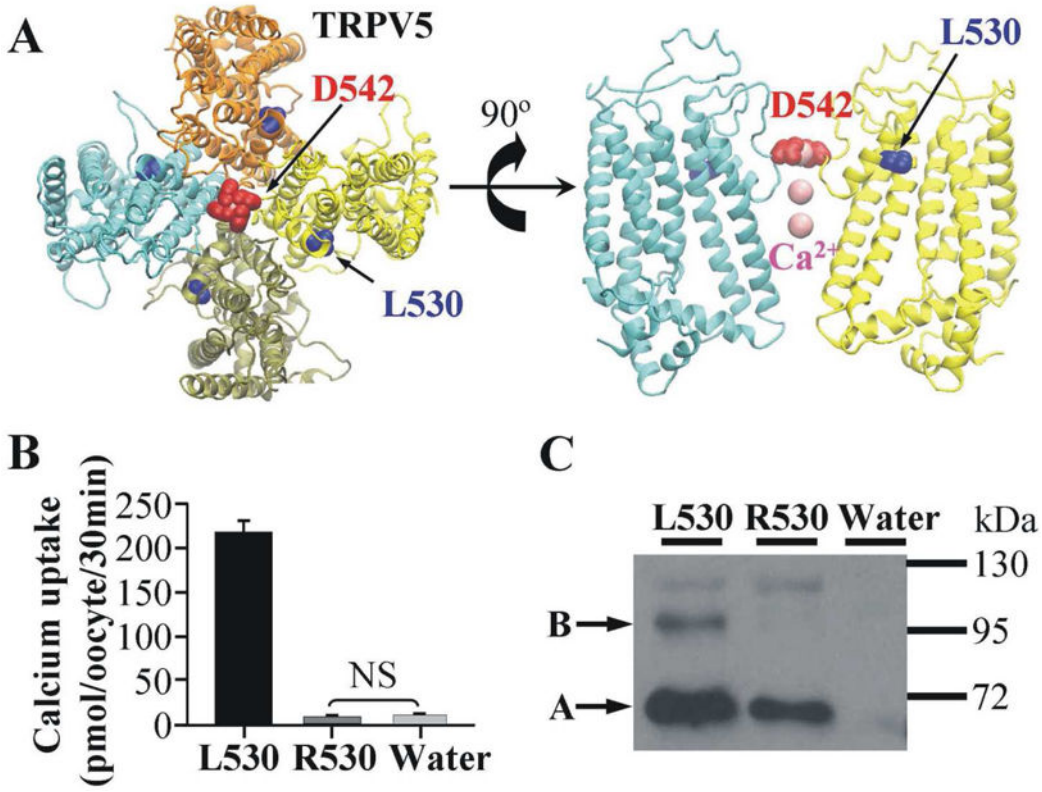

Fig. 1. The L530R variation abolishes the Ca^{2+} uptake activity of TRPV5

(A) The location of L530 in the modeled structure of the TRPV5 tetramer. The top view of the TRPV5 tetramer is shown on the left and only two monomers are shown in the side view (right panel) for clarity. The four monomers are shown in cyan, tan, yellow and orange, respectively. D542 in the Ca^{2+} selective filter, L530 where variation occurred, and Ca^{2+} ions are shown in red, blue and pink, respectively. **(B)** Ca^{2+} uptake in *Xenopus* oocytes expressing TRPV5 with L530, R530, or in control oocytes. Each group contained Ca^{2+} uptake values of 18 *Xenopus* oocytes from two frogs. NS means the difference is not significant. **(C)** Western blot analysis of TRPV5 variants (L530 and R530) expressed in *Xenopus* oocytes. Band B represents complex-glycosylated form of TRPV5, and band A represents core-glycosylated form.

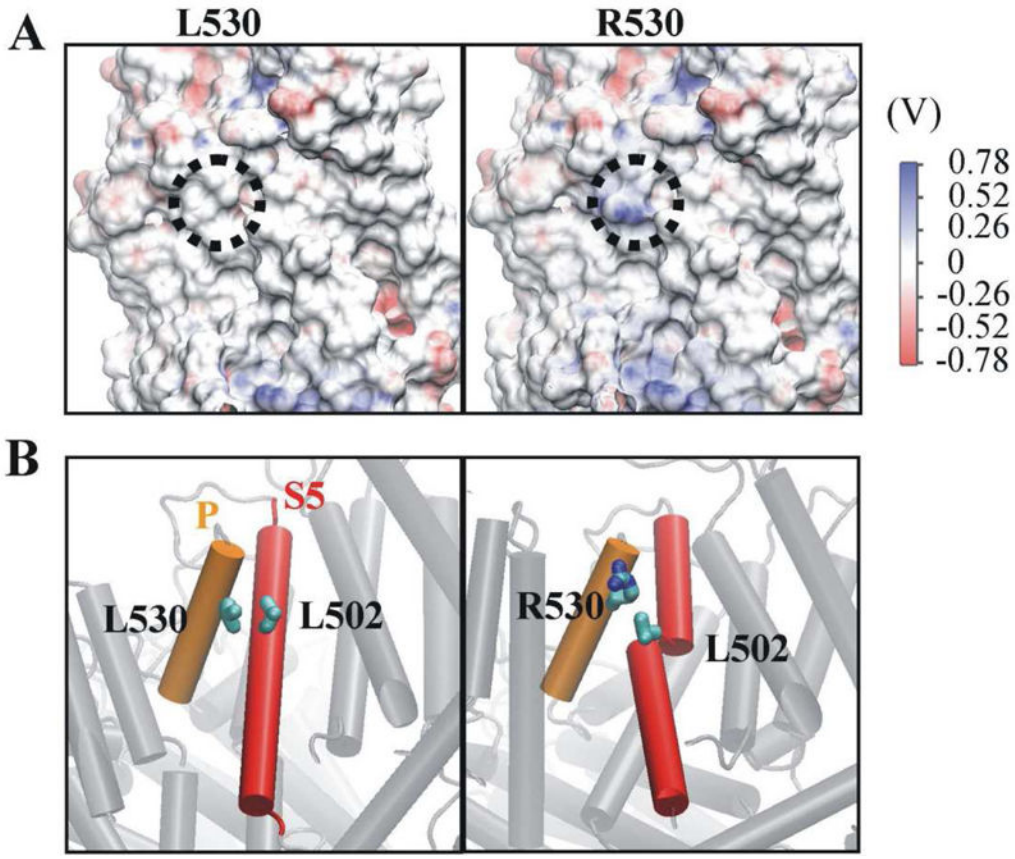

Fig. 2. The L530R variation changes electrostatic potential at position 530 and damages the secondary structure of transmembrane helix 5

(A) The electrostatic potential of residue 530 (dotted circle) shifted positively when L530 was replaced by R530. **(B)** Transmembrane helix 5 (S5) broke into two helices in the R530 variant as a result of the disruption of the interaction between R530 and L502. The pore helix (P) and S5 are shown in orange and red, respectively. The carbon and nitrogen atoms of residue 530 are labeled in cyan and blue, respectively. For clarity, the hydrogen atoms of residue 530 are not shown.

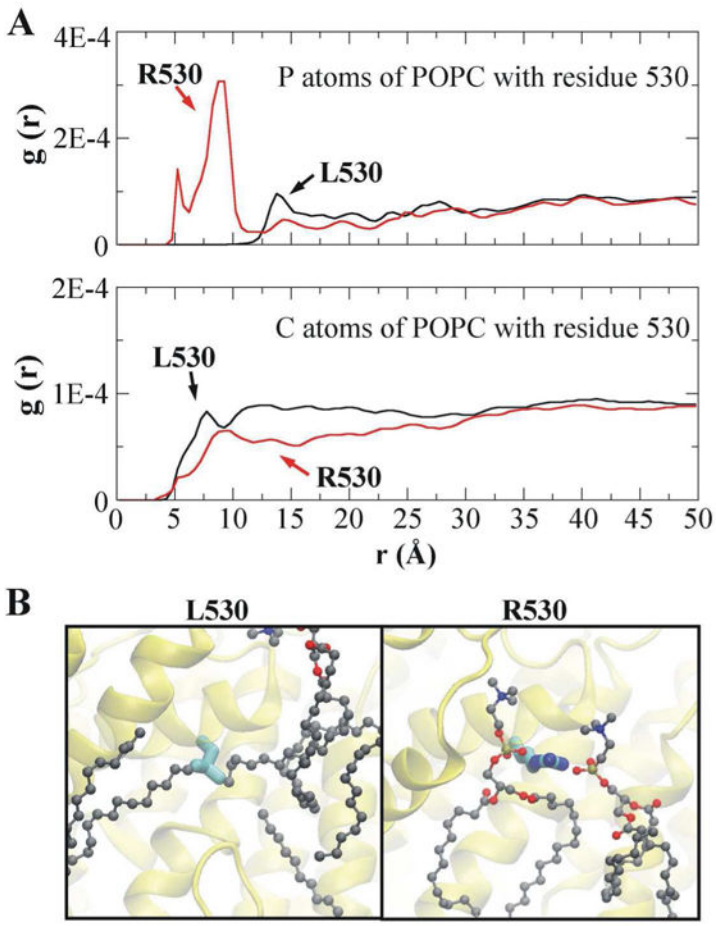

Fig. 3. The L530R variation alters the interaction between residue 530 and lipid molecules

(A) Radial distribution functions (RDFs) of residue 530 with phosphorus (P) atoms (upper panel) and carbon (C) atoms (lower panel) of POPC lipids. **(B)** Simulation snapshots showing the coordination of residue 530 with the surrounding lipid molecules. The P, C, O (oxygen) and N (nitrogen) atoms of POPC are shown in tan, gray, red and blue, respectively. The labelling of atoms in residue 530 is the same as in Fig. 2B.

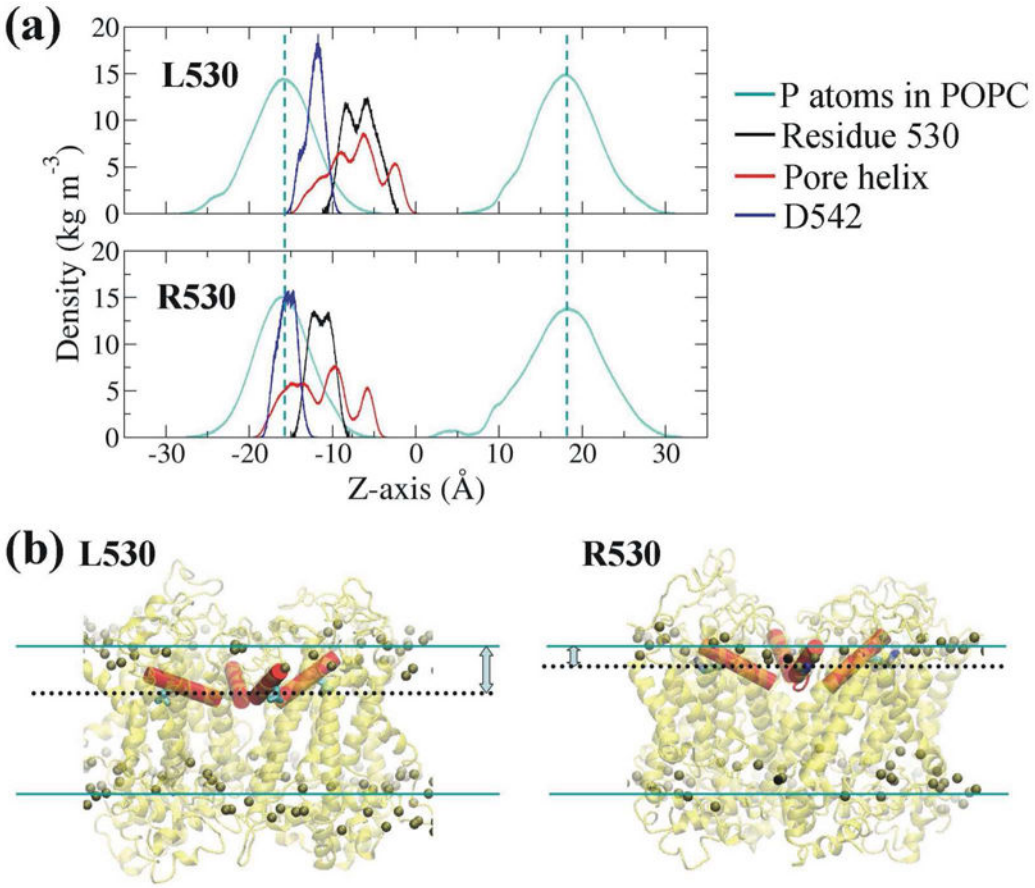

Fig. 4. The L530R variation causes a shift of the pore helix and residue D542 towards the membrane surface

(A) Comparison of the mass density of residue 530, pore helix and residue D542 between **L530** and **R530** systems. The dashed cyan lines indicate the density peaks of the P atoms of POPC lipids. Note the density values of P atoms of POPC and pore helix are reduced 40 times and 10 times, respectively, in order to be shown in the same scale. **(B)** Final structures showing the position of residue 530 (black dotted lines) and pore helix (in red) relative to membrane surface (cyan lines). The P atoms of POPC are shown as balls.